show that in this region, N decreases exponentially along the axis with an e-folding length $l_N \simeq 100$ μm, while its transverse variation remains small within the focal spot. If one chooses $l = l_N$, then expression (14) gives $(\theta_D)_{\min} \simeq 3.6°$. The effective value of l is probably somewhat smaller, however, on account of the finite length of the focal waist. It is difficult to estimate accurately the resulting correction to l because of the uncertainty of where the backscatter originated, but it is probable that l lies in the range 50–100 μm. We therefore obtain $(\theta_D)_{\min} \simeq 3.6°$–$5.1°$, in reasonable agreement with the ~2° resolution estimated from the burnpaper data. A more definitive test of this theory would proceed along lines similar to the phase-conjugation experiments in liquids;[6,7] i.e., impose a phase-aberration plate near the lens, and attempt to observe the phase compensation in the backscatter.

In summary, I have suggested that ray retracing in laser-plasma backscatter arises from the same physical mechanism believed to cause phase conjugation in stimulated backscatter from liquids, and I have generalized this theory to include inhomogeneity of the active medium.

The author wishes to acknowledge the rather valuable contributions from S. E. Bodner, J. F. Reintjes, and B. H. Ripin. This work is sponsored by the U. S. Department of Energy.

[1]K. Eidmann and R. Sigel, in *Laser Interaction and Related Plasma Phenomena*, edited by H. J. Schwarz and Heinrich Hora (Plenum, New York, 1974), Vol. 3B, p. 667; J. A. Stamper *et al.*, *ibid.*, p. 713; C. Patou, Opt. Commun. 18, 97 (1976).

[2]B. H. Ripin, F. C. Young, J. A. Stamper, C. M. Armstrong, R. Decoste, E. A. McLean, and S. E. Bodner, Phys. Rev. Lett. 39, 611 (1977); B. H. Ripin, Naval Research Laboratory Memorandum Report No. 3684, 1977 (unpublished).

[3]S. E. Bodner and J. L. Eddleman, Lawrence Livermore Laboratory Report No. 73378, 1971 (unpublished); C. S. Liu and P. K. Kaw, in *Advances in Plasma Physics*, edited by P. K. Kaw, W. L. Kruer, C. S. Liu, and K. Nishikawa (Wiley, New York, 1976), Vol. 6, p. 83.

[4]D. W. Phillion, W. L. Kruer, and V. C. Rupert, Phys. Rev. Lett. 39, 1529 (1977); C. L. Tang, J. Appl. Phys. 37, 2945 (1966).

[5]I. M. Bel'dyugin, M. G. Galushkin, E. M. Zemskov, and V. I. Mandrosov, Sov. J. Quantum Electron. 6, 1349 (1976).

[6]B. Ya. Zel'dovich, V. I. Popovichev, V. V. Ragul'skii, and F. S. Faizullov, Pis'ma Zh. Eksp. Teor. Fiz. 15, 160 (1972) [JETP Lett. 15, 109 (1972)]; O. Yu. Nosach, V. I. Popovichev, V. V. Ragul'skii, and F. S. Faizullov, Pis'ma Zh. Eksp. Teor. Fiz. 16, 617 (1972) [JETP Lett. 16, 435 (1972)]; V. I. Bespalov, A. A. Betin, and G. A. Pasmanik, Pis'ma Zh. Tekh. Fiz. 3, 215 (1977) [Sov. Tech. Phys. Lett. 3, 85 (1977)]; V. Wang and C. R. Guiliano, Opt. Lett. 2, 4 (1978).

[7]B. Ya. Zel'dovich, N. A. Mel'nikov, N. F. Pilipetskii, and V. V. Ragul'skii, Pis'ma Zh. Eksp. Teor. Fiz. 25, 41 (1977) [JETP Lett. 25, 36 (1977)]; A. I. Sokolovskaya, G. L. Brekhovskiskli, and A. D. Kudryautseva, Opt. Commun. 24, 74 (1978).

[8]V. G. Sidorovich, Zh. Tekh. Fiz. 46, 2168 (1976) [Sov. Phys. Tech. Phys. 21, 1270 (1976)]; B. Ya. Zel'dovich and V. V. Shkunov, Sov. J. Quantum Electron. 7, 610 (1977); V. B. Gerasimov, S. A. Gerasimova, and V. K. Orlov, Sov. J. Quantum Electron. 7, 527 (1977).

[9]H. Kogelnik, Bell System Tech. J. 48, 2909 (1969).

Filamentation Instability of Ion Beams Focused in Pellet-Fusion Reactors

R. F. Hubbard and D. A. Tidman
Institute for Physical Science and Technology, University of Maryland, College Park, Maryland 20742
(Received 5 July 1978)

The growth of current filamentation instability is calculated for intense multi-GeV heavy-ion beams focused across a target chamber onto a fusion pellet. Conditions for which this instability growth can be kept small are given.

High-power beams of multi-GeV heavy ions have been considered as possible igniters for pellet fusion.[1,2] The conditions under which these beams would be subject to filamentation instability in the target-chamber gas are explored.[2-4]

A typical member of the beam system must be accurately focused across a target chamber of radius ~10 m onto a pellet of radius a few millimeters. As the heavy-ion pulse advances towards the pellet it undergoes stripping and multiple scattering, and ionizes the background gas. The resulting plasma conductivity gives rise to a return current that neutralizes the beam cur-

rent to within a few percent (complete neutralization is assumed below in treating the growth of current filaments). This result is based on a beam-propagation code containing classical transport coefficients,[5] i.e., microinstabilities are assumed to be suppressed by background gas collisions.[2] The upper limit for the target-chamber gas density is set by multiple scattering (e.g., in propagating 10 m through air at 10 Torr a 30-GeV U beam has a minimum focal-spot radius of 0.34 cm).

We find that filamentation can be avoided within acceptable parameter ranges by increasing either the beam-injection radius, emittance, or number of beams used to deliver a given total power. If, however, the instability is allowed to occur, simulation studies[6] suggest that it may rapidly provide transverse thermal energy to the beam and prevent focusing.

The plasma in the reactor chamber consists of background electrons and ions produced by ionization of the background gas, plus beam ions moving with velocity V_b. Each component of the plasma is assumed to be Maxwellian with a drift or beam velocity V_j in the z direction and thermal velocities v_{jx} and v_{jz} perpendicular and parallel to the beam. For most cases of interest to us the background gas is sufficiently dense (0.1–10 Torr) that the collision frequency ν_{ei} between background electrons and ions is much larger than typical filamentation growth rates. The background plasma is thus treated using fluid equations, while the beam is treated as collisionless.

For $\vec{k}=k\hat{x}$, $\vec{B}=B\hat{y}$, and $\vec{E}=E\hat{z}$ in a field-free region the resulting dispersion relation then follows as

$$0=k^2c^2-\omega^2+\omega_b^2\left[1-\left(\frac{V_b^2+v_{bz}^2}{v_{bx}^2}\right)[1+\xi_b Z(\xi_b)]\right]-\frac{4\pi i\omega\sigma}{1-4\pi i\omega\sigma/\omega_e^2}. \tag{1}$$

Here ω_e and ω_b are the electron plasma frequency and beam plasma frequency, $\omega=\omega_r+i\gamma$ is the complex wave frequency, k is the wave number, $\xi_b=\omega/\sqrt{2}kv_{bx}$, σ is the conductivity,[7] and $Z(\xi_b)=(1/\sqrt{\pi})\times\int_{-\infty}^{\infty}dt\exp(-t^2)/(t-\xi_b)$ is the plasma dispersion function.

Equation (1) has unstable solutions ($\gamma>0$) only for $\omega_r=0$ (purely growing modes) and $k<k_0\approx\omega_b V_b/cv_{bx}$. The last term in Eq. (1) replaces the background plasma contributions to the collisionless dispersion relation given by Davidson *et al.*[3] The background electron stream velocity, which can play a dominant role in the collisionless case, no longer appears in the dispersion relation.

If the beam has a constant radial density out to a distance r, ω_b can be rewritten

$$\omega_b=(4e^2/m_b)^{1/2}N_b^{1/2}Z_b/r, \tag{2}$$

where the beam density per unit length N_b remains constant. As a focused beam approaches the pellet, Z_b increases as electrons are stripped from the beam ions while r decreases rapidly. Thus, ω_b may increase by several orders of magnitude from its value at injection, and rapid instability growth may occur. Z_b is primarily determined by the background gas density and propagation distance. We have assumed a charge-stripping model for uranium suggested by Yu *et al.*[8] to estimate Z_b.

To estimate the beam radius $r(z)$, we use an envelope equation derived by Lee and Cooper.[9] If the beam is sufficiently well current neutralized, self-pinch effects can be neglected, and the envelope equation can be integrated analytically. For a flat radial beam profile,

$$r^2=r_0^2-\frac{2r_0^2z}{s}+\left[\left(\frac{r_0V_b}{s}\right)^2+2\Delta_{b0}^2\right]\frac{z^2}{V_b^2}+\frac{8\pi\hbar c^4z^3}{3\lambda_R^e De^2V_b^3}\left(\frac{m_eZ_b}{m_b\gamma_r}\right)^2. \tag{3}$$

Here r_0 is the beam radius at injection, $\Delta v_b^2=(V^2-2\dot{r}^2)$, V^2 is the mean-square transverse velocity, s is the chamber radius, λ_R^e is the electron radiation length (3×10^4 cm for air), and $D=760/p$(Torr). The equations in Ref. 9 have been transformed using $z=V_bt$ and $r=\sqrt{2}R$, and $\gamma_r\equiv(1-V_b^2/c^2)^{-1/2}$.

The residual velocity Δv_b^2 in the envelope equation is approximately equal to the beam transverse thermal velocity v_{bx}^2 in the dispersion relation. It is related to the emittance[9] $E^2=2\gamma_r^2r^2\Delta v_b^2$. E^2 is essentially constant for a focused heavy-ion beam.[9] Hence,

$$\Delta v_b(z)=\Delta v_{b0}\,r_0/r(z). \tag{4}$$

For a well-focused beam, $\dot{r}_0^2=(-r_0V_b/s)^2\gg(\Delta v_{b0})^2$. As the beam appraoches the pellet, the beam transverse thermal velocity increases rapidly according to Eq. (4), and $\Delta v_b\approx\dot{r}_0/\sqrt{2}$ at the pellet.

This transverse heating of the beam plays a major role in reducing $\gamma(k)$ near the pellet. If v_{bx} is replaced by Δv_b, the term in Eq. (1) proportional to $\omega_b V_b/v_{bx} \approx k_0 c$ is independent of r; the r^{-1} dependence of ω_b in Eq. (2) is balanced by the r^{-1} dependence of Δv_b in Eq. (4). As r approaches its minimum value $r_{\min}$ at the pellet, v_{bx} is usually sufficiently large that $|\xi_b| \ll 1$. Neglecting displacement current, the growth rate is

$$\gamma(k) = \frac{kc^2(k_0^2 - k^2)}{4\pi k\sigma + (\pi/2)^{1/2} k_0^2 c^2/\Delta v_b} = k\left\{\frac{4e^2 N_b}{m_b}\left(\frac{Z_b V_0}{\Delta v_{b0} r_0}\right)^2 - k^2c^2\right\}\left[4\pi k\sigma + 4\left(\frac{\pi}{2}\right)^{1/2}\frac{e^2 N_b}{m_b}\left(\frac{Z_b V_b}{\Delta v_{b0} r_0}\right)\left(\frac{r}{r_0 \Delta v_{b0}}\right)\right]^{-1}. \quad (5)$$

From Eq. (5), the wave number k^* of the fastest growing mode is estimated using Newton's method.

Since $\vec{k} \cdot \vec{V}_b = 0$ in this analysis, the unstable waves do not propagate with the beam. Instead, unstable growth at any position z begins at $t = t_0$ when the head of the beam arrives at z and ceases at $t = t_0 + \tau_p$, where τ_p is the pulse length. Hence, the number of e foldings in the electromagnetic field amplitudes is given by $N_\gamma(k^*; z) = \gamma(k^*; z)\tau_p$, assuming that the beam parameters of the pulse passing through a fixed z are constant. If $\gamma(k^*; z)$ is sufficiently small so that $N_\gamma \lesssim 5$–10, field amplitudes will never grow large enough for filamentation to become a problem.

We now search for model parameters which allow the beam to be focused over a distance of several meters to a radius $r_{\min} \lesssim 0.1$ cm, while keeping N_γ sufficiently small. Maximum growth almost always occurs at the pellet where $r = r_{\min}$ and $\Delta v_b \approx \dot{r}_0/\sqrt{2}$. Based on beam-transport-code results,[5] we choose $V_b = c/2$. $T_e = 20$ eV and $2n_e = n_0 =$ the initial neutral-gas density. For $N_b = 3 \times 10^{11}$ cm^{-1}, the beam energy and power are 34 GeV and 25 TW. Since at least 100 TW are required for pellet fusion, the parameters are applicable for a multibeam reactor. The pulse length is 10 ns. The pressure p, initial radius r_0, initial beam thermal spread Δv_{b0}, and the chamber radius s must also be specified. Equation (3) determines $r(z)$. The full dispersion relation [Eq. (1)] is solved numerically although the approximations leading to Eq. (5) are usually satisfied.

Figure 1 plots N_γ at $z = s$ for a 10-ns, 25-TW beam as a function of r_0 with $p = 1$ Torr. We choose $\Delta v_{b0}/V_b = 1.4 \times 10^{-4}$ for $s = 5$ m and 4×10^{-5} for $s = 10$ m, so that $r_{\min} = 0.10$ cm in both cases. At $z \approx s$ and $r \approx r_{\min}$, the second term in the denominator of Eq. (5) is usually negligible, so that $\gamma \sim r_0^{-2}$. Figure 1 clearly reflects this scaling. Serious problems with filamentation may occur for $r_0 \lesssim 10$ cm, although pinch effects play an increasingly important role[5] for small r_0.

Figure 2 shows the importance of the initial beam thermal spread Δv_{b0}. Again, $p = 1$ Torr, and the curves are for $r_0 = 20$ cm, $s = 5$ m and $r_0 = 40$ cm, $s = 10$ m. Serious filamentation growth may occur for $\Delta v_{b0}/V_b \lesssim 2 \times 10^{-5}$ since $\gamma \sim (\Delta v_{b0}/V_b)^{-2}$ while $r_{\min}$ may become unacceptably large for $\Delta v_{b0}/V_b \gtrsim 2 \times 10^{-4}$.

If V_b is constant, beam power is proportional to N_b. Figure 3 reveals that $\gamma \sim N_b \sim P$ as expected from Eq. (5). Parameters are the same as in Fig. 1 with $r_0 = 20$ and 40 cm for $s = 5$ and 10 m, respectively. For a 5-m target chamber, single beam power in excess of 500 TW may be employed without encountering adverse filamentation.

As the pressure increases, $r_{\min}$ increases due to multiple scattering while Z_b (and hence γ) increases due to enhanced charge stripping. Seri-

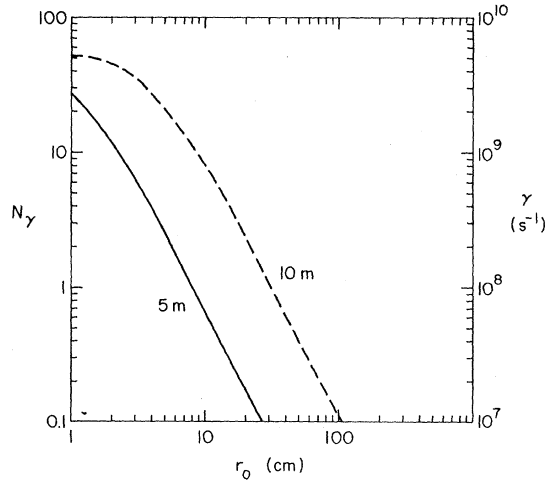

FIG. 1. Number of e foldings N_γ (or equivalently, growth rate γ) vs initial beam radius r_0 for a 10-ns uranium-beam pulse. Other parameters are $V_b = c/2$, $P = 25$ TW, $p = 1$ Torr, $T_e = 20$ eV, and $n_e = \frac{1}{2} n_0$. The focal-spot radius $r_{\min} = 0.10$ cm is achieved by setting $\Delta v_{b0}/V_b = 1.4 \times 10^{-4}$ for a target-chamber radius of 5 m and $\Delta v_{b0}/V_b = 4 \times 10^{-5}$ for a 10-m chamber. The growth rate is for the fastest growing mode at the location of the pellet. The beam strips to a charge state of 69 after traveling 5 m, and $Z_b = 76$ after 10 m. Defocusing due to filamentation instability may occur for $N_\gamma \gtrsim 5$. Therefore, a large initial beam radius is desirable since $\gamma \sim r_0^{-2}$.

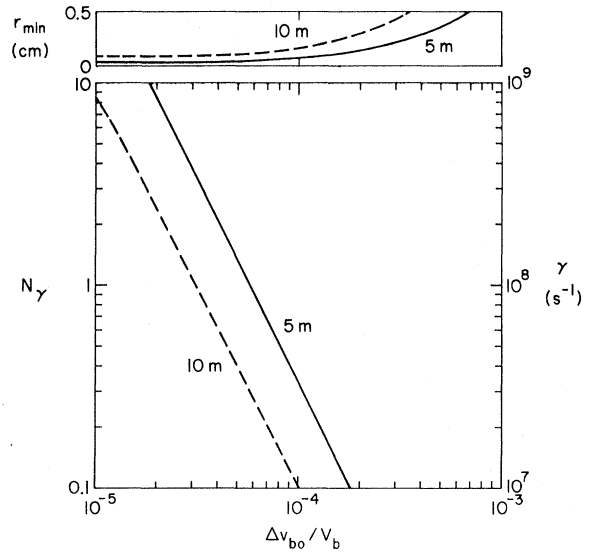

FIG. 2. $N_\gamma = \gamma\tau_p$ vs the initial transverse beam thermal spread $\Delta v_{b0}/V_b$ for $\tau_p = 10$ ns. The initial beam radius $r_0 = 20$ cm for $s = 5$ m and is 40 cm for a 10-m chamber. Other parameters are same as in Fig. 1. Since $\gamma \sim (\Delta_{b0}/V_b)^{-2}$, the initial thermal spread should be as large as possible while meeting the requirements for r_{min} dictated by the pellet size.

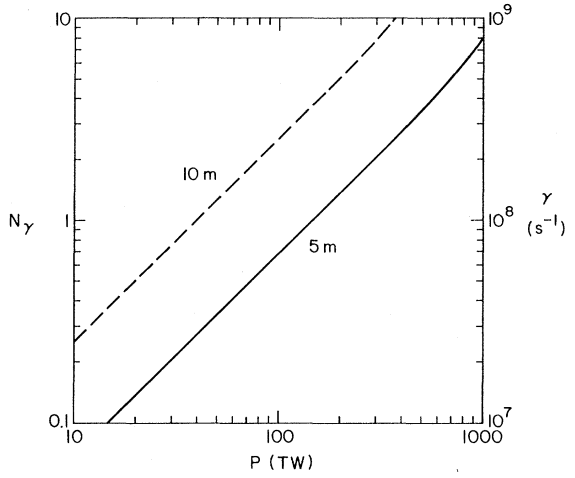

FIG. 3. N_γ vs beam power P assuming $V_b = c/2$ (34 GeV). Again, $r_0 = 20$ and 40 cm for $s = 5$ and 10 m, respectively, with other parameters as in Fig. 1. As expected from Eq. (5), $\gamma \sim N_b \sim P$. If $s = 5$ m, one may be able to avoid filamentation defocussing (i.e., $N_\gamma < 5$) with a 0.1-cm pellet for single beam power as high as 700 TW. However, it is clearly desirable to reduce the power or current carried by a single beam and employ a multiple-beam system.

ous two-stream instability problems may exist below 1 Torr[5] while r_{min} may be unacceptably high at high pressures.

Unlike the $k_z = 0$ modes we have investigated, modes with $k_z \neq 0$ will have $\omega_r \neq 0$ and may propagate in the direction of the beam. We believe the nonpropagating modes to be the most important ones for filamentation since preliminary studies indicate that propagating modes usually have small group velocities and hence do not convect with the beam.

In conclusion, we have shown that for a wide variety of parameters appropriate to a heavy-ion fusion reactor chamber, filamentation instabilities will not grow to amplitudes significantly above the initial noise level. Strategies for reducing growth rates are apparent from Eq. (5) and Figs. 1–3. Perhaps the easiest way to control filamentation is to inject the beam with a large initial radius so that the transverse beam temperature near the pellet is large. It is also advantageous to increase the initial transverse beam thermal spread as large as focusing requirements allow or to decrease beam power and use multibeam systems. Filamentation growth may be significantly lower at pressures below 1 Torr, but higher pressures may be required to suppress electrostatic two-stream instabilities. Finally, control of filamentation instabilities will be significantly easier if somewhat larger pellets (allowing larger r_{min}) can be used or if the target-chamber radius can be minimized.

We are grateful to Dr. M. Rosenbluth who emphasized the possible importance of this instability to us. Useful discussions with Dr. D. Spicer and Dr. E. Lee are also gratefully acknowledged. This work was supported in part by the U. S. Department of Energy, Contract No. EY-76-S-05-5000.

[1]Lawrence Berkeley Laboratory, Report No. 5543, July 1976, edited by R. O. Baumgarter, W. B. Herrmannsfeldt, D. L. Judd, and L. Smith (unpublished).

[2]Brookhaven National Laboratory Report No. 50769, 1977, edited by L. Smith (unpublished).

[3]R. C. Davidson, D. A. Hammer, I. Haber, and C. E. Wagner, Phys. Fluids 15, 317 (1972).

[4]C. G. Callen, Jr., R. F. Dashen, R. L. Garwin, R. A. Muller, B. Richter, and M. N. Rosenbluth, SIR International Report No. JSR-77-41, 1978 (unpublished).

[5]D. Spicer, D. A. Tidman, and R. F. Hubbard, "Propagation of High Current Particle Beams through Gases" (to be published). See also Ref. 2 pp. 52 and 55 for

similar results.

[6]R. Lee and M. Lampe, Phys. Rev. Lett. 31, 1390 (1973).

[7]S. I. Braginskii, in *Reviews of Plasma Physics*, edited by M. A. Leontovich (Consultants Bureau, New York, 1965), Vol. 5, p. 216.

[8]S. S. Yu, H. L. Buchanan, F. W. Chambers, and E. P. Lee, Ref. 2, p. 55.

[9]E. P. Lee and R. K. Cooper, Part. Accel. 7, 83 (1976).

Influence of Toroidal Effects on the Stability of the Internal Kink Mode

R. M. O. Galvão, P. H. Sakanaka, and H. Shigueoka

Instituto de Física "Gleb Wataghin," Universidade Estadual de Campinas, 13.100 Campinas, São Paulo, Brazil

(Received 17 May 1978)

Using the σ-stability technique, we study the stability of the internal kink mode in toroidal geometry. We show that there are two unstable regions separated by a stable one in a β-q_c stability diagram. In one of these regions toroidal effects are stabilizing and in the other they are destabilizing. Discrepant results of previous analytical theories and experimental results are explained.

The internal kink mode has been the object of intense theoretical research recently[1-6] because of its relevance to the triggering mechanism of internal disruptions in tokamak discharges.[7-11] In a cylindrical plasma column of length $2\pi R_0$ and radius a with an equilibrium magnetic field $(0, B_\theta(r), B_z(r))$, the mode is excited when $q(r) = rB_z(r) < 1$ in some region inside the plasma; the mode poloidal and toroidal wave numbers are $m = 1$ and $|n| = 1$, respectively.

Two different analytical theories have been developed for the internal kink mode in toroidal geometry so far.[4-6] The one developed by Bussac *et al.*[4,5] is based upon the energy principle. According to their results, the toroidal effects are stabilizing if

$$\beta_p^* = [2/B_\theta^2(r_0)] \int_0^{r_0} (r/r_0)^2 (-dp/dr)\, dr$$

is below some critical value; $p(r)$ is the plasma pressure. The theory developed by Pao[6] is based upon a normal-mode analysis. He uses $\epsilon = a/R_0$ and r_0/a as expansion parameters; here r_0 is the radius where $q(r_0) = 1$. According to Pao's theory, the internal kink mode is *not* stabilized by toroidal effects, as predicated by Bussac *et al.* To our knowledge, the discrepancy between the two theories has not been elucidated yet.

Experimental results have shown the presence of the $m = |n| = 1$ instability superimposed on the sawtooth oscillations characteristic of the internal disruptions.[10,11] The TFR group's results indicate also that the $m = |n| = 1$ oscillations vanish when the plasma density is increased.[10] Since this corresponds to an increase in the plasma pressure, this result is somewhat surprising and not explained by previous theories. Using the σ-stability technique,[12] we show that in toroidal geometry there are stable and unstable regions for the $m = 1$ internal mode in the β-q_c parameter space, as found by Freidberg and co-workers for the external kink mode.[13] Here we define $\beta = p(0)/[p(0) + \frac{1}{2}B_T^2(0)]$, $q_c = q(0)$, and $B_T(0)$ is the toroidal component of the equilibrium magnetic field $B(r)$ at the magnetic axis. The apparent discrepancy between the two analytical theories and the experimental result described above are explained on the basis of the β-q_c stability diagrams. We also calculate the mode spectrum for different values of β.

Copenhaver[14] has derived a simple σ Euler equation starting from a theory of the magnetohydrodynamic spectrum in toroidal geometry developed by Goedbloed.[15] The relevant equations are flux averaged and expanded in powers of ϵ. Copenhaver's equation, with first-order toroidal terms included, is

$$\frac{d}{dr}\left[f(r)\frac{d}{dr}(r\xi)\right] - g_M(r)(r\xi) = 0, \qquad (1)$$

where

$$f(r) = N/rD, \quad N = (\rho\sigma^2 + F^2)[\rho\sigma^2(\gamma p + B^2) + \gamma p F^2],$$

$$D = \rho^2\sigma^4 + \rho\sigma^2(m^2/r^2 + n^2/R^2)(\gamma p + B^2) + (m^2/r^2 + n^2/R^2)\gamma p F^2,$$